*Mathematical Biosciences and Engineering*

https://www.aimspress.com/journal/mbe

MBE, 21(4): 5283–5307.
DOI: 10.3934/mbe.2024233
Received: 12 December 2023
Revised: 20 February 2024
Accepted: 29 February 2024
Published: 06 March 2024

*Research article*

# Analysis of a COVID-19 model with media coverage and limited resources

**Tao Chen, Zhiming Li* and Ge Zhang**

College of Mathematics and System Science, Xinjiang University, Urumqi 830017, China

* **Correspondence:** Email: zmli@xju.edu.cn.

**Abstract:** The novel coronavirus disease (COVID-19) pandemic has profoundly impacted the global economy and human health. The paper mainly proposed an improved susceptible-exposed-infected-recovered (SEIR) epidemic model with media coverage and limited medical resources to investigate the spread of COVID-19. We proved the positivity and boundedness of the solution. The existence and local asymptotically stability of equilibria were studied and a sufficient criterion was established for backward bifurcation. Further, we applied the proposed model to study the trend of COVID-19 in Shanghai, China, from March to April 2022. The results showed sensitivity analysis, bifurcation, and the effects of critical parameters in the COVID-19 model.

**Keywords:** SEIR epidemic model; limited medical resources; media coverage; vaccination; backward bifurcation

## 1. Introduction

The COVID-19 is an acute respiratory infectious disease caused by SARS-CoV-2 virus. The main transmissions are direct, aerosol, and contact. The clinical manifestations of confirmed cases are fever, fatigue, dry cough, and a few patients with upper airway symptoms such as nasal congestion and runny nose. In severe cases, the infection can lead to pneumonia, acute respiratory syndrome, renal failure, and even death [1]. With the mobility of human beings, the COVID-19 epidemic soon spread around the world, causing a significant impact on the global economy and human health. According to the World Health Organization (WHO), as of September 14, 2023, there are 770,563,467 confirmed cases worldwide, of which 6,957,216 are confirmed deaths [2]. The continued spread of COVID-19 threatens human health. Given this, a deeper understanding of COVID-19 is necessary. As an effective tool, mathematical modeling plays a crucial role in studying COVID-19 transmission and control strategies. Since Kermack and McKendrick [3] first used the theory of the ordinary differential equation (ODE) to study the dynamics of the epidemic, many important models have been proposed based on the transmission and pathogenicity of the disease in the past 100 years, such as susceptible-infected-

recovered (SIR) [4–6], susceptible-infected-recovered-susceptible (SIRS) [7–9], susceptible-infected-susceptible (SIS) [10, 11], susceptible-infected-recovered-infected (SIRI) [12], SEIR models [13, 14], and so on [15–17]. These models have been extended to study the spread of COVID-19 from different perspectives, for example, the epidemiological dynamics [18–20], transmission characteristic [21, 22], clinical classification [23], and prevention and control strategies [24].

However, most of the models mentioned above often ignore the impact of media coverage and share a common assumption that medical resources are sufficient, which is often not valid in practice. In the early stages of the epidemic, due to a lack of understanding of the disease, biomedical interventions are insufficient to protect people from disease invasion. Thanks to the increasingly developed internet, radio, and television technology, media coverage is a convenient, fast, and effective measure to curb the spread of disease. The most frequently used method is to inform people of nonpharmacological interventions [25, 26]. Studies suggest that media coverage dramatically influences people's behaviors [27–29]. Under the guidance of media publicity, people gradually pay attention to diseases and take necessary preventive measures to reduce the possibility of infection [30]. Maji et al. [31] considered a COVID-19 model with social media campaigns. Khajanchi et al. [32] showed that media coverage had a positive influence in controlling COVID-19 spreading during the initial phase of the epidemic. In general, infectious diseases are typically transmitted through direct contact between susceptible and infected individuals. Let $S(t)$ and $I(t)$ be the numbers of susceptible and infectious individuals at time $t$, respectively. Because of the media coverage, the direct contact rate decreases. Based on this point, Li and Cui [11] proposed a contact transmission rate, denoted by $\mathcal{B}(I(t))$, to describe the effect of the media coverage as follows:

$$\mathcal{B}(I(t)) = \beta_1 - \frac{\beta_2 I(t)}{\alpha + I(t)},$$

where $\beta_1$ is the usual contact rate without the media coverage, $\beta_2$ is the maximum contact rate that the media coverage can reduce, and $\alpha$ ($> 0$) is a constant to reflect the speed with which people react to the media coverage. The contact rate reaches its minimum $\beta_1 - \beta_2$ when $I(t) \to +\infty$. Since the media coverage cannot make the disease extinct, it is reasonable to assume that $\beta_1 - \beta_2 > 0$ [13]. Compared with the classical contact rates, $\mathcal{B}(I(t))$ can reflect the inhibitory effect of media coverage on the spread of infectious diseases. Thus, a nonlinear incidence with the media coverage is expressed by

$$g(S(t), I(t)) = \mathcal{B}(I(t))S(t)I(t) = \left(\beta_1 - \frac{\beta_2 I(t)}{\alpha + I(t)}\right) S(t)I(t).$$

On the other hand, medical resources are often limited during the epidemic. For example, some nations and regions have successively experienced material shortages at the beginning of the COVID-19 outbreak. To explore the influence of limited medical resources, Wang and Ruan [33] first proposed a piecewise treatment function $h(I) = r$ if $I > 0$, otherwise 0. Here, $r$ represents the saturation level of medical resources. Further, Wang [34] modified the treatment function, that is, if $0 \le I \le I_0$, then $h(I) = rI$, and if $I > I_0$, then $h(I) = rI_0$. It means that before the medical resources reach saturation, the cure rate is proportional to the number of infected individuals. After the medical resources reach saturation, the cure rate remains at the $rI_0$ and does not increase with the increase in the number of infected individuals. However, the above two treatment functions are not differentiable everywhere. To overcome this limitation, Zhang and Liu [35] provided a treatment function

$$h(I(t)) = \frac{cI(t)}{1 + bI(t)},$$

where $b$ ($\geq 0$) is the saturation factor measuring the impact of delayed treatment on infected individuals and $c$ ($> 0$) is the cure rate. It is easy to verify that $h(I(t))$ can be approximated by $cI(t)$ when $I(t)$ is small. That is to say, the function $h(I)$ characterizes the limited medical resources in that the cure rate is proportional to the number of infected individuals. In contrast, when the number of infected individuals is large, the cure rate reaches a saturation level of $c/b$. The item $1/(1 + bI)$ describes the reverse effect of the infected individuals being delayed for treatment. In addition, when $b = 0$, $h(I)$ degenerates into the linear form.

According to the above analysis, some of the studies focused on media coverage, while some concentrated on limited medical resources. However, there are few types of research on both media coverage and limited resources. Moreover, the COVID-19 vaccine is also a powerful way and should be considered in the model. Motivated by this, this paper aims to design a new epidemic model with vaccination for reflecting not only the impact of media coverage, but also limited medical resources on the spread of COVID-19. The rest of the paper is organized as follows. We first present the SEIR model with media coverage and limited medical resources in Section 2, then we analyze the model theoretically in Section 3. We use daily confirmed, cured, cumulative, and existing cases in Shanghai from March to April 2022 as an application. The numerical simulations for COVID-19 data are carried out to explore the inhibitory effect of media reports, medical resources, and vaccination on the transmission of COVID-19 in Section 4. A brief conclusion is given in the last section.

## 2. Model formulation

Since the human body is not immediately contagious after COVID-19, the individuals often become infected after incubation. Divide the total population $N(t)$ into four classes: susceptible, exposed, infected, and recovered individuals. The number of people in these four classes at time $t$ is denoted by $S(t)$, $E(t)$, $I(t)$, and $R(t)$, respectively. Combined with the fact that the virus has an incubation period, it is more suitable for the SEIR model to describe the spread of COVID-19.

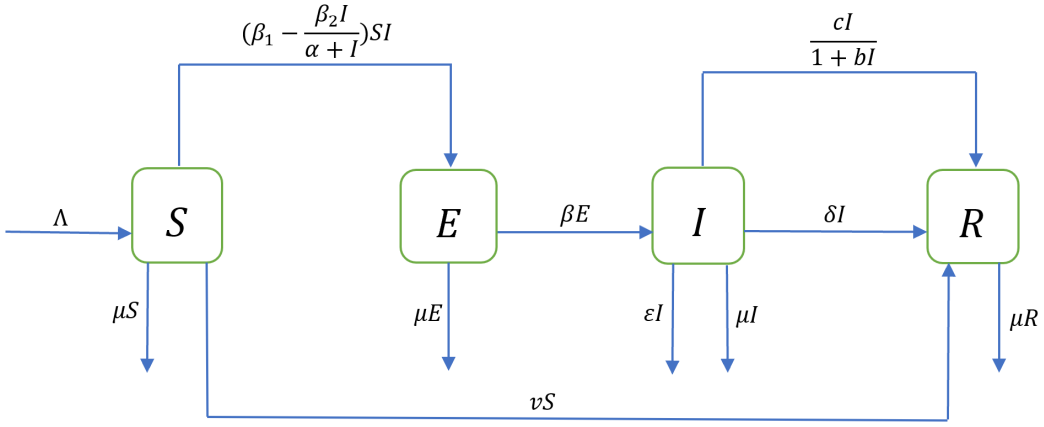


**Figure 1.** The compartmental chart of an improved SEIR model.

As mentioned above, the media coverage and limited medical resources are two factors that cannot be ignored in the spread of COVID-19. However, as far as we know, the research about the epidemic model with media coverage and limited medical resources is still an opening problem. As an extension

of the above results, an improved SEIR model with media coverage, limited medical resources, and vaccination is proposed as follows:

$$\begin{cases} \mathrm{d}S(t) = \left[\Lambda - (\mu + v)S(t) - \left(\beta_1 - \dfrac{\beta_2 I(t)}{\alpha + I(t)}\right) S(t)I(t)\right] \mathrm{d}t, \\ \mathrm{d}E(t) = \left[\left(\beta_1 - \dfrac{\beta_2 I(t)}{\alpha + I(t)}\right) S(t)I(t) - (\beta + \mu)E(t)\right] \mathrm{d}t, \\ \mathrm{d}I(t) = \left[\beta E(t) - (\varepsilon + \delta + \mu)I(t) - \dfrac{cI(t)}{1 + bI(t)}\right] \mathrm{d}t, \\ \mathrm{d}R(t) = \left[\delta I(t) - \mu R(t) + \dfrac{cI(t)}{1 + bI(t)} + vS(t)\right] \mathrm{d}t. \end{cases} \tag{2.1}$$

The meanings of all parameters assumed to be nonnegative in the model are listed in Table 1. The compartmental chart of the model is shown in Figure 1. Although $\delta I$ and $\frac{cI(t)}{1+bI(t)}$ both flow from the compartment $I$ to $R$, $\delta I$ is the self-healing of infected individuals, while $\frac{cI(t)}{1+bI(t)}$ represents the recovery of infected individuals through hospital treatment.

**Table 1.** Definition of parameters in the model (2.1).

| Parameter | Definition |
|---|---|
| $\Lambda$ | Recruitment rate of susceptible individuals |
| $\mu$ | Natural mortality rate |
| $\varepsilon$ | Disease-related mortality rate |
| $\beta_1$ | Usual contact rate without media alert |
| $\beta_2$ | Maximum contact rate that can be reduced by the media coverage |
| $v$ | Vaccination rate |
| $\alpha$ | A constant that reflects the speed with which people react to the media coverage |
| $b$ | Saturation factor measuring the impact of delayed treatment |
| $c$ | Cure rate |
| $\beta$ | Prevalence rate of exposed individuals |
| $\delta$ | Recovery rate |

Since the first three equations are independent of the fourth equation, the model (2.1) can be simplified as

$$\begin{cases} \mathrm{d}S(t) = \left[\Lambda - (\mu + v)S(t) - \left(\beta_1 - \dfrac{\beta_2 I(t)}{\alpha + I(t)}\right) S(t)I(t)\right] \mathrm{d}t, \\ \mathrm{d}E(t) = \left[\left(\beta_1 - \dfrac{\beta_2 I(t)}{\alpha + I(t)}\right) S(t)I(t) - (\beta + \mu)E(t)\right] \mathrm{d}t, \\ \mathrm{d}I(t) = \left[\beta E(t) - (\varepsilon + \delta + \mu)I(t) - \dfrac{cI(t)}{1 + bI(t)}\right] \mathrm{d}t. \end{cases} \tag{2.2}$$

To facilitate calculation and representation, let $\phi_1 = \mu + v$, $\phi_2 = \beta + \mu$, and $\phi_3 = \varepsilon + \delta + \mu$. The

model (2.2) then can be equivalently represented as

$$\begin{cases} \mathrm{d}S(t) = \left[\Lambda - \phi_1 S(t) - \left(\beta_1 - \dfrac{\beta_2 I(t)}{\alpha + I(t)}\right) S(t) I(t)\right] \mathrm{d}t, \\ \mathrm{d}E(t) = \left[\left(\beta_1 - \dfrac{\beta_2 I(t)}{\alpha + I(t)}\right) S(t) I(t) - \phi_2 E(t)\right] \mathrm{d}t, \\ \mathrm{d}I(t) = \left[\beta E(t) - \phi_3 I(t) - \dfrac{cI(t)}{1 + bI(t)}\right] \mathrm{d}t. \end{cases} \tag{2.3}$$

## 3. Basic properties

In this section, some basic properties of model (2.1) are provided to illustrate its epidemiological meaning.

### *3.1. Positivity and boundedness*

**Theorem 1.** If the initial value $(S(0), E(0), I(0), R(0))$ is nonnegative, then the solution $(S(t), E(t), I(t), R(t))$ of the model (2.1) is nonnegative for all $t \in [0, +\infty)$.

*Proof.* Since the solution is continuous concerning the initial value, we only need to prove that for any positive initial value $(S(0), E(0), I(0), R(0))$, the solution $(S(t), E(t), I(t), R(t))$ of model (2.1) is also positive for all $t \in (0, +\infty)$. From the first equation of model (2.1), we have

$$\frac{\mathrm{d}S(t)}{\mathrm{d}t} > -\left[(\mu + v) + \left(\beta_1 - \frac{\beta_2 I(t)}{\alpha + I(t)}\right) I(t)\right] S(t).$$

Hence, as $S(0) > 0$, we directly get that $S(t) > 0$ for all $t \in [0, +\infty)$.

Next, define $\chi(t) = \min\{S(t), E(t), I(t), R(t)\}$. Clearly, $\chi(0) = \min\{S(0), E(0), I(0), R(0)\} > 0$. To prove the theorem, we only need to prove that $\chi(t) > 0$ for all $t \in [0, +\infty)$. Suppose there exists a moment $t_0$ such that $\chi(t) > 0$ when $t \in [0, t_0)$ and $\chi(t_0) = 0$, then the following three cases need to be considered: (i) $\chi(t_0) = E(t_0)$; (ii) $\chi(t_0) = I(t_0)$; and (iii) $\chi(t_0) = R(t_0)$.

Let $\chi(t_0) = E(t_0)$. Since $\chi(t) > 0$ when $t \in [0, t_0)$, then from the second equation of model (2.1), we have

$$\frac{\mathrm{d}E(t)}{\mathrm{d}t} > -(\beta + \mu)E(t) \quad \text{for all} \quad t \in [0, t_0).$$

According to the comparison principle, one gets that $E(t) > E(0)e^{-(\beta+\mu)t}$, $t \in [0, t_0)$. Letting $t \to t_0$ yields $0 = E(t_0) > E(0)e^{-(\beta+\mu)t_0} > 0$, which is a contradiction. Similarly, we can also derive the contradiction in cases (ii) and (iii). Therefore, the solution of model (2.1) is positive for all $t \in [0, +\infty)$.

**Theorem 2.** The solution $(S(t), E(t), I(t), R(t))$ of model (2.1) are bounded.

*Proof.* Adding all the four equations of (2.1) yields

$$\frac{\mathrm{d}N}{\mathrm{d}t} = \Lambda - \mu N - \varepsilon I \le \Lambda - \mu N.$$

Thus, $\limsup_{t \to +\infty} N \le \frac{\Lambda}{\mu}$, that is, the $(S(t), E(t), I(t), R(t))$ of the model (2.1) are bounded.

Furthermore, according to the comparison theorem, one can obtain that $N(t) \leq (N(0)-\Lambda/\mu)e^{-\mu t}+\Lambda/\mu$, then $N(t) \leq \Lambda/\mu$ if $N(0) \leq \Lambda/\mu$. Thus, the positively invariant region of model (2.1) is

$$\Omega = \left\{(S, E, I, R) \in \mathbb{R}_+^4 : S + E + I + R \leq \frac{\Lambda}{\mu}\right\}.$$

By the way, if $N(0) > \Lambda/\mu$, then $N(t) \leq N(0)$.

### *3.2. Disease-free equilibrium (DFE) and its local stability*

The model (2.3) is equivalent to the model (2.1). For convenience, we consider the model (2.3) in the following. Clearly, the model (2.3) always exists a DFE $P_0 = (\Lambda/\phi_1, 0, 0)$.

The basic reproduction number, denoted by $\mathscr{R}_0$, is a vital threshold in the epidemic model and determines whether the epidemic breaks out. There is more than one way to calculate the basic reproduction number, and the most common method is the next-generation matrix method. Denote by $F$ and $V$ the new infection compartment and transition terms of model (2.3), respectively, then

$$F = \begin{bmatrix} F_E \\ F_I \end{bmatrix} = \begin{bmatrix} \left(\beta_1 - \frac{\beta_2 I}{\alpha+I}\right) S I \\ 0 \end{bmatrix}, \quad V = \begin{bmatrix} V_E \\ V_I \end{bmatrix} = \begin{bmatrix} \phi_2 E \\ \phi_3 I + \frac{cI}{1+bI} - \beta E \end{bmatrix}.$$

The Jacobian matrix for the infection components $E$ and $I$ at the DFE $P_0$ are, respectively, given by

$$\mathcal{F} = \mathcal{D}F(P_0) = \begin{bmatrix} \frac{\partial F_E}{\partial E}|_{P_0} & \frac{\partial F_E}{\partial I}|_{P_0} \\ \frac{\partial F_I}{\partial E}|_{P_0} & \frac{\partial F_I}{\partial I}|_{P_0} \end{bmatrix} = \begin{bmatrix} 0 & \frac{\beta_1\Lambda}{\phi_1} \\ 0 & 0 \end{bmatrix},$$
$$\mathcal{V} = \mathcal{D}V(P_0) = \begin{bmatrix} \frac{\partial V_E}{\partial E}|_{P_0} & \frac{\partial V_E}{\partial I}|_{P_0} \\ \frac{\partial V_I}{\partial E}|_{P_0} & \frac{\partial V_I}{\partial I}|_{P_0} \end{bmatrix} = \begin{bmatrix} \phi_2 & 0 \\ -\beta & \phi_3 + c \end{bmatrix},$$

then the basic reproduction number for model (2.3) is

$$\mathscr{R}_0 = \rho(\mathcal{F}\mathcal{V}^{-1}) = \frac{\beta_1\beta\Lambda}{\phi_1\phi_2(\phi_3 + c)}.$$

Next, the local stability of the DFE $P_0$ will be studied. To begin with, model (2.3) is linearized at $P_0$ by using the Jacobian matrix as follows

$$\mathcal{J}(P_0) = \begin{bmatrix} -\phi_1 & 0 & -\frac{\beta_1\Lambda}{\phi_1} \\ 0 & -\phi_2 & \frac{\beta_1\Lambda}{\phi_1} \\ 0 & \beta & -(\phi_3 + c) \end{bmatrix}.$$

It has negative eigenvalues, if and only if, $\beta_1\beta\Lambda < \phi_1\phi_2(\phi_3 + c)$, i.e., $\mathscr{R}_0 < 1$. Given the above discussion, the following stability criterion is derived.

**Theorem 3.** The DFE $P_0$ of model (2.3) is locally asymptotically stable if $\mathscr{R}_0 < 1$, and unstable if $\mathscr{R}_0 > 1$.

*3.3. Existence of the endemic equilibrium point (EEP)*

The EEP $P^*(S^*, E^*, I^*)$ of model (2.3) can be given by letting

$$\begin{cases} 0 = \Lambda - \phi_1 S - \left(\beta_1 - \dfrac{\beta_2 I}{\alpha + I}\right) S I, \\ 0 = \left(\beta_1 - \dfrac{\beta_2 I}{\alpha + I}\right) S I - \phi_2 E, \\ 0 = \beta E - \phi_3 I - \dfrac{cI}{1 + bI}, \end{cases}$$

which equals to

$$\begin{cases} S = \dfrac{\phi_2 E}{(\beta_1 - \frac{\beta_2 I}{\alpha + I})I}, \\ E = \dfrac{\phi_3 I + \frac{cI}{1+bI}}{\beta}, \\ 0 = \Lambda - \phi_1 S - \left(\beta_1 - \dfrac{\beta_2 I}{\alpha + I}\right) S I. \end{cases} \tag{3.1}$$

Denote

$$G = \frac{\beta_1\phi_1(\phi_3 + c) + b\alpha\beta_1\phi_1\phi_3 + \alpha\beta_1^2(\phi_3 + c)}{\phi_1(\phi_3 + c)(\beta_1 - \beta_2 + \alpha b\beta_1)},$$
$$K = \frac{1}{\beta_1}(\beta_1 - \beta_2 + \alpha b\beta_1)\phi_1\phi_2(\phi_3 + c).$$

Substituting $S$ and $E$ into the third equality of (3.1) yields an equation of the form

$$AI^3 + BI^2 + CI + D = 0, \tag{3.2}$$

where

$$\begin{aligned} A =& (\beta_1 - \beta_2)b\phi_2\phi_3, \\ B =& -(\beta_1 - \beta_2)\beta b\Lambda + (\beta_1 - \beta_2)\phi_2(\phi_3 + c) + \alpha\beta_1 b\phi_2\phi_3 + b\phi_1\phi_2\phi_3, \\ C =& -(\beta_1 - \beta_2 + \alpha\beta_1 b)\beta\Lambda + \phi_1\phi_2(\phi_3 + c) + b\alpha\phi_1\phi_2\phi_3 + \alpha\beta_1\phi_2(\phi_3 + c), \\ =& \frac{1}{\beta_1}(\beta_1 - \beta_2 + \alpha b\beta_1)\phi_1\phi_2(\phi_3 + c)(G - \mathscr{R}_0) \\ =& K(G - \mathscr{R}_0), \\ D =& -\alpha\beta_1\beta\Lambda + \phi_1\phi_2\alpha(\phi_3 + c) = \phi_1\phi_2\alpha(\phi_3 + c)(1 - \mathscr{R}_0). \end{aligned}$$

It is obvious that $A > 0$; $C > 0 \Leftrightarrow \mathscr{R}_0 < G$; $D > 0 \Leftrightarrow \mathscr{R}_0 < 1$, and $G = 1$ equals to

$$b = \frac{(\phi_3 + c)(\phi_1\beta_2 + \alpha\beta_1^2)}{\phi_1\alpha\beta_1 c} := b^*.$$

Furthermore, it is decreasing for $G$ with respect to $b$.

Let $\Delta := q^2/4 + p^3/27$ be the discriminant of (3.2), where $p = (3AC - B^2)/(3A^2)$ and $q = (27A^2D - 9ABC + 2B^3)/(27A^3)$, then the existence of the equilibria is summarized as the following result.

**Theorem 4.** (I) When $0 \le b \le b^*$, the following results hold.

(i) If $\mathscr{R}_0 > G$ or $1 < \mathscr{R}_0 < G$ and $B > 0$, the model (2.3) has a unique EEP.
(ii) If $\mathscr{R}_0 < 1$ and $B > 0$, the model (2.3) has no EEP.
(iii) If $1 < \mathscr{R}_0 < G$, $B < 0$ and $\Delta < 0$, the model (2.3) has three EEPs.
(iv) If $\mathscr{R}_0 < 1$ and $B < 0$, then
  (iv1) when $\Delta < 0$, there are two EEPs of the model (2.3);
  (iv2) when $\Delta > 0$, there is no EEP of the model (2.3);
  (iv3) when $\Delta = 0$ and $\mathscr{R}_0 > G - \frac{B^2}{3AK}$, there is an EEP of the model (2.3).

(II) When $b > b^*$, the following results hold.
(i) If $\mathscr{R}_0 > 1$, the model (2.3) has an EEP.
(ii) If $G < \mathscr{R}_0 < 1$, then
  (ii1) when $\Delta < 0$, there are two EEPs of the model (2.3);
  (ii2) when $\Delta > 0$, there is no EEP of the model (2.3);
  (ii3) when $\Delta = 0$, there is an EEP of the model (2.3).
(iii) If $\mathscr{R}_0 < G$ and $B > 0$, the model (2.3) has no EEP.
(iv) If $\mathscr{R}_0 < G$ and $B < 0$, then
  (iv1) when $\Delta < 0$, there are two EEPs of the model (2.3);
  (iv2) when $\Delta > 0$, there is no EEP of the model (2.3);
  (iv3) when $\Delta = 0$, there is an EEP of the model (2.3).

*Proof.* The theorem can be proved using Descartes' rule of signs. Let

$$f(I) := AI^3 + BI^2 + CI + D.$$

For the conclusion (I)(i), when $0 \le b \le b^*$, we have $G > 1$. Since $\mathscr{R}_0 > G \ge 1$, we get $C < 0$ and $D < 0$. $f(I)$ only changes sign once whether $B > 0$ or $B < 0$. Hence, from Descartes' rule of signs, it has a real positive root and model (2.3) has an EEP. If $1 < \mathscr{R}_0 < G$ and $B > 0$, then $C > 0$ and $D < 0$. In this case, $f(I)$ changes sign once, too, then the model (2.3) has an EEP. Conclusion (I)(i) is then proved. The proofs of conclusions (I)(ii), (II)(i), and (II)(iii) are similar to conclusion (I)(i) and then omitted.

Next, we prove the conclusions (I)(iii) and (I)(iv).

1) The condition $1 < \mathscr{R}_0 < G$ yields $C > 0$ and $D < 0$. Combined with $B < 0$, $f(I)$ changes its sign three times, meaning that it may have three positive roots or one positive root. On the other hand, $f(-I) = -AI^3 + BI^2 - CI + D$, which does not change the sign, then $f(I)$ has no negative root. Furthermore, $\Delta < 0$ follows that $f(I)$ has three different real roots. Hence, $f(I)$ has three different positive real roots, which means that model (2.3) has three EEPs. Conclusion (I)(iii) is then proved.

2) If $\mathscr{R}_0 < 1$ and $B < 0$, $f(I)$ then changes sign twice and $f(-I)$ changes sign once, which means $f(I)$ has a negative root. Further, if $\Delta < 0$, then $f(I)$ has two positive roots and one negative root, indicating that model (2.3) has two EEPs. If $\Delta > 0$, only one negative root indicates that the model (2.3) has no EEP. If $\mathscr{R}_0 > G - \frac{B^2}{3AK}$, then $B^2 - 3AC > 0$. Combining with $\Delta = 0$, $f(I)$ has a positive double root, which indicates that model (2.3) has an EEP. It completes the proof of (I)(iv). The proofs of several other conclusions are similar, so we omit them.

According to Theorem 4, Tables 2 and 3 show the distribution of EEP of the model (2.3) under $0 \le b \le b^*$ and $b > b^*$, respectively.

**Table 2.** Real positive roots for $0 \le b \le b^*$, depending on the sign of $B, C, D$ and $\Delta$.

| Cases | $B$ | $C$ | $D$ | The number of real positive roots |
|---|---|---|---|---|
| (i) $\mathscr{R}_0 > G$ | $+(-)$ | $-$ | $-$ | 1 |
| or $1 < \mathscr{R}_0 < G$ | $+$ | $+$ | $-$ | 1 |
| (ii) $\mathscr{R}_0 < 1$ | $+$ | $+$ | $+$ | 0 |
| (iii) $1 < \mathscr{R}_0 < G$ | $-$ | $+$ | $-$ | 3 if $\Delta < 0$ |
| | $-$ | $+$ | $+$ | 2 if $\Delta < 0$ |
| (iv) $\mathscr{R}_0 < 1$ | $-$ | $+$ | $+$ | 0 if $\Delta > 0$ |
| | $-$ | $+$ | $+$ | 1 if $\Delta = 0$ and $\mathscr{R}_0 > G - \frac{B^2}{3AK}$ |

**Table 3.** Real positive roots for $b > b^*$ depending on the sign of $B, C, D$ and $\Delta$.

| Cases | $B$ | $C$ | $D$ | The number of real positive roots |
|---|---|---|---|---|
| (i) $\mathscr{R}_0 > 1$ | $+(-)$ | $-$ | $-$ | 1 |
| | $+(-)$ | $-$ | $+$ | 2 if $\Delta < 0$ |
| (ii) $G < \mathscr{R}_0 < 1$ | $+(-)$ | $-$ | $+$ | 0 if $\Delta > 0$ |
| | $+(-)$ | $-$ | $+$ | 1 if $\Delta = 0$ |
| (iii) $\mathscr{R}_0 < G$ | $+$ | $+$ | $+$ | 0 |
| | $-$ | $+$ | $+$ | 2 if $\Delta < 0$ |
| (iv) $\mathscr{R}_0 < G$ | $-$ | $+$ | $+$ | 0 if $\Delta > 0$ |
| | $-$ | $+$ | $+$ | 1 if $\Delta = 0$ |

**Remark 1.** In Theorem 4, $b$ is an important parameter that determines the distribution of the equilibria of the model. If $b = 0$, (3.2) degenerates to

$$\bar{B}I^2 + \bar{C}I + D = 0, \tag{3.3}$$

where

$$\begin{aligned}
\bar{B} =& (\beta_1 - \beta_2)\phi_2(\phi_3 + c),\\
\bar{C} =& \frac{1}{\beta_1}(\beta_1 - \beta_2)\phi_1\phi_2(\phi_3 + c)(\bar{G} - \mathscr{R}_0),\\
\bar{G} =& \frac{\beta_1\phi_1 + \alpha\beta_2^2}{\phi(\beta_1 - \beta_2)}.
\end{aligned}$$

Note that $\bar{B}$ is larger than zero and $\bar{G}$ is larger than unity. Hence, if $\mathscr{R}_0 < 1$, all coefficients of Eq (3.3) are positive and there is no positive root, which means that there is no EEP in this case. If $\mathscr{R}_0 > 1$, then $D < 0$. Whether $\bar{C}$ is greater than zero or not, there always exists a unique positive root of the equation, which means that there exists a unique EEP. If $\mathscr{R}_0 = 1$, then $D = 0$ and $\bar{C} > 0$, there is unique positive root of (3.3) $I = -\bar{C}/\bar{B} < 0$, and the model has no EEP. Therefore, when $b = 0$, a forward bifurcation exhibits in model (2.3), which is consistent with Theorem (4) (I)(i).

### 3.4. Locally asymptotical stability of EEP

In Theorem 4 (I)(i),(ii), and (II)(i), the model (2.3) has a unique EEP $P^*(S^*, E^*, I^*)$. This subsection aims to investigate the locally asymptotical stability of $P^*$. Denote

$$H := \frac{\phi_2\ (c+\phi_3+b\,\phi_3 I^*)\left((\beta_1-\beta_2)(I^{*2}+2\alpha I^*)+\alpha^2\beta_1\right)}{\beta\ (\alpha+I^*)\ (1+bI^*)\ (\beta_1 I^*-\beta_2 I^*+\alpha\beta_1)} > 0.$$

**Theorem 5.** The model (2.3) has a unique EEP, which is locally asymptotically stable if $\mathscr{R}_0 > 1$,

$$\phi_2\left(\phi_1+\frac{(\beta_1-\beta_2)I^*+\beta_1\alpha}{\alpha+I^*}I^*\right)\left(\phi_3+\frac{c}{(1+bI^*)^2}\right) > \beta H\phi_1,$$

and

$$\begin{aligned}&\left[\phi_1+\phi_2+\phi_3+\frac{c}{(1+bI^*)^2}+\frac{(\beta_1-\beta_2)I^*+\beta_1\alpha}{\alpha+I^*}I^*\right]\left[\left(\phi_2+\phi_3+\frac{c}{(1+bI^*)^2}\right)\right.\\&\left.\times\left(\phi_1+\frac{(\beta_1-\beta_2)I^*+\beta_1\alpha}{\alpha+I^*}I^*\right)+\phi_2\left(\frac{c}{(1+bI^*)^2}+\phi_3\right)-\beta H\right]+\beta H\phi_1\\&>\phi_2\left(\phi_1+\frac{(\beta_1-\beta_2)I^*+\beta_1\alpha}{\alpha+I^*}I^*\right)\left(\phi_3+\frac{c}{(1+bI^*)^2}\right).\end{aligned}$$

*Proof.* The Jacobian matrix $\mathcal{J}(P^*)$ of the model (2.3) is given by

$$\mathcal{J}(P^*)=\begin{bmatrix}-\phi_1-\frac{(\beta_1-\beta_2)I^*+\beta_1\alpha}{\alpha+I^*}I^* & 0 & -H\\ \frac{(\beta_1-\beta_2)I^*+\beta_1\alpha}{\alpha+I^*}I^* & -\phi_2 & H\\ 0 & \beta & -\frac{c}{(1+bI^*)^2}-\phi_3\end{bmatrix}.$$

Through calculation, the characteristic equation of $\mathcal{J}(P^*)$ is

$$\lambda^3+a_1\lambda^2+a_2\lambda+a_3=0,$$

where

$$\begin{aligned}a_1=&\phi_1+\phi_2+\phi_3+\frac{c}{(1+bI^*)^2}+\frac{(\beta_1-\beta_2)I^*+\beta_1\alpha}{\alpha+I^*}I^*,\\a_2=&\left(\phi_2+\phi_3+\frac{c}{(1+bI^*)^2}\right)\left(\phi_1+\frac{(\beta_1-\beta_2)I^*+\beta_1\alpha}{\alpha+I^*}I^*\right)\\&+\phi_2\left(\frac{c}{(1+bI^*)^2}+\phi_3\right)-\beta H,\\a_3=&\phi_2\left(\phi_1+\frac{(\beta_1-\beta_2)I^*+\beta_1\alpha}{\alpha+I^*}I^*\right)\left(\phi_3+\frac{c}{(1+bI^*)^2}\right)-\beta H\phi_1.\end{aligned}$$

Note that $a_1 > 0$ and $a_3 > 0$ whenever

$$\phi_2\left(\phi_1+\frac{(\beta_1-\beta_2)I^*+\beta_1\alpha}{\alpha+I^*}I^*\right)\left(\phi_3+\frac{c}{(1+bI^*)^2}\right) > \beta H\phi_1.$$

Furthermore,

$$\begin{aligned}\Delta' &= a_1a_2 - a_3\\ &= \left[\phi_1 + \phi_2 + \phi_3 + \frac{c}{(1+bI^*)^2} + \frac{(\beta_1-\beta_2)I^* + \beta_1\alpha}{\alpha + I^*}I^*\right]\\ &\quad\times\left[\left(\phi_2 + \phi_3 + \frac{c}{(1+bI^*)^2}\right)\left(\phi_1 + \frac{(\beta_1-\beta_2)I^* + \beta_1\alpha}{\alpha + I^*}I^*\right)\right.\\ &\quad\left.+\ \phi_2\left(\frac{c}{(1+bI^*)^2} + \phi_3\right) - \beta H\right] - \phi_2\left(\phi_1 + \frac{(\beta_1-\beta_2)I^* + \beta_1\alpha}{\alpha + I^*}I^*\right)\\ &\quad\times\left(\phi_3 + \frac{c}{(1+bI^*)^2}\right) + \beta H\phi_1.\end{aligned}$$

Therefore, combining with the Routh-Hurwitz criterion, the EEP $P^*$ of the model (2.3) is locally asymptotically stable.

### *3.5. The backward bifurcation*

According to Theorem 4, the model (2.3) may exhibit a bifurcation for the values of $\mathscr{R}_0$ when $G < \mathscr{R}_0 < 1$. Next, following Theorem 4 in [36], we look for the parameter conditions that lead to the backward bifurcation. Letting $\mathscr{R}_0 = 1$ yields $\beta_1 = \beta_1^* := \frac{\phi_1\phi_2(\phi_3+c)}{\beta\Lambda}$. Denote $\hat{b} = \frac{\alpha\phi_1\phi_2^2(\phi_3+c)^2 + 2\beta_2\Lambda^2\beta^2}{2\alpha\Lambda\beta c\phi_1\phi_2}$.

**Theorem 6.** The model (2.3) has a backward bifurcation at $\mathscr{R}_0 = 1$ when $b > \hat{b}$.

*Proof.* Let $x_1 = S$, $x_2 = E$ and $x_3 = I$, then the model (2.3) becomes

$$\begin{cases}\dfrac{\mathrm{d}x_1}{\mathrm{d}t} = \Lambda - \phi_1 x_1 - \left(\beta_1 - \dfrac{\beta_2 x_3}{\alpha + x_3}\right)x_1x_3 =: f_1,\\ \dfrac{\mathrm{d}x_2}{\mathrm{d}t} = \left(\beta_1 - \dfrac{\beta_2 x_3}{\alpha + x_3}\right)x_1x_3 - \phi_2 x_2 := f_2,\\ \dfrac{\mathrm{d}x_3}{\mathrm{d}t} = \beta x_2 - \phi_3 x_3 - \dfrac{cx_3}{1+bx_3} := f_3.\end{cases}$$

Suppose $\beta_1$ is the bifurcation parameter. When $\beta_1 = \beta_1^*$, the Jacobian matrix of the model (2.3) at $P_0(\Lambda/\phi_1, 0, 0)$ is

$$\mathcal{J}(P_0, \beta_1^*) = \begin{bmatrix}-\phi_1 & 0 & -\frac{\phi_2(\phi_3+c)}{\beta}\\ 0 & -\phi_2 & \frac{\phi_2(\phi_3+c)}{\beta}\\ 0 & \beta & -(\phi_3+c)\end{bmatrix}.$$

The eigenvalues of $\mathcal{J}(P_0, \beta_1^*)$ are $\lambda_1 = 0, \lambda_2 = -\phi_1$, and $\lambda_3 = -\phi_2 - (\phi_3 + c)$. Obviously, $\lambda_2 < 0$, $\lambda_3 < 0$, and $\lambda_1$ is a simple zero eigenvalue of $\mathcal{J}(P_0, \beta_1^*)$.

The right eigenvector of $\mathcal{J}(P_0, \beta_1^*)$ for $\lambda_1 = 0$ is denoted by $\boldsymbol{w} = (w_1, w_2, w_3)^\top$, then

$$\boldsymbol{w} = \begin{bmatrix}w_1\\ w_2\\ w_3\end{bmatrix} = \begin{bmatrix}-\frac{\phi_2(\phi_3+c)}{\phi_1}\\ \phi_3 + c\\ \beta\end{bmatrix},$$

which is from $\mathcal{J}(P_0,\beta_1^*)\boldsymbol{w}=0$. Moreover, the left eigenvector $\boldsymbol{v}=(v_1,v_2,v_3)$ meeting $\boldsymbol{v}\cdot\boldsymbol{w}=1$ can be found by

$$\begin{cases} -\phi_1 v_1 = 0, \\ -\phi_2 v_2 + \beta v_3 = 0, \\ \dfrac{\phi_2(\phi_3+c)}{\phi_1} v_2 - (\phi_3+c)v_3 = 0. \end{cases}$$

Hence, $\boldsymbol{v}=(0,\frac{1}{\phi_2+\phi_3+c},\frac{\phi_2}{\beta(\phi_2+\phi_3+c)})$. Evaluating the partial derivatives at $P_0$, we have

$$\begin{aligned} &\frac{\partial^2 f_1}{\partial x_1\partial x_3} = -\frac{\phi_1\phi_2(\phi_3+c)}{\Lambda\beta}, \quad \frac{\partial^2 f_1}{\partial x_3^2} = \frac{2\Lambda\beta_2}{\alpha\phi_1}, \quad \frac{\partial^2 f_1}{\partial x_3\partial\beta_1} = -\frac{\Lambda}{\phi_1}, \\ &\frac{\partial^2 f_2}{\partial x_1\partial x_3} = \frac{\phi_1\phi_2(\phi_3+c)}{\Lambda\beta}, \quad \frac{\partial^2 f_2}{\partial x_3^2} = -\frac{2\Lambda\beta_2}{\alpha\phi_1}, \quad \frac{\partial^2 f_2}{\partial x_3\partial\beta_1} = \frac{\Lambda}{\phi_1}, \\ &\frac{\partial^2 f_3}{\partial x_3^2} = 2bc, \end{aligned}$$

and other partial derivatives equal to zero. Thus,

$$\begin{aligned} \boldsymbol{a} &= \sum_{i,j,k}^{3} v_k w_i w_j \frac{\partial^2 f_k}{\partial x_i \partial x_j}(P_0,\beta_1^*) \\ &= -\frac{\phi_2^2(\phi_3+c)^2}{\Lambda(\phi_2+\phi_3+c)} - \frac{2\Lambda\beta_2\beta^2}{\alpha\phi_1(\phi_2+\phi_3+c)} + \frac{2bc\phi_2\beta}{\phi_2+\phi_3+c}, \\ \boldsymbol{b} &= \sum_{k,i}^{3} v_k w_i \frac{\partial^2 f_k}{\partial x_i\partial\beta_1}(P_0,\beta_1^*) = \frac{\Lambda\beta}{\phi_1(\phi_2+\phi_3+c)}. \end{aligned}$$

Obviously, $\boldsymbol{b}>0$. When $b>\hat{b}$, $\boldsymbol{a}>0$. Therefore, the model (2.3), when $b>\hat{b}$, exhibits a backward bifurcation at $\mathscr{R}_0=1$.

**Remark 2.** Combining Theorems 4 and 6, we note that parameter $b$ determines not only the existence of EEP, but also the bifurcation of the model (2.3).

**Remark 3.** The existence of backward bifurcation suggests that the disease may persist even if we make the basic reproduction number less than 1. This makes it more difficult to control the epidemic. From the proof of Theorem 6, we note that the timely treatment of infected individuals is an essential factor for backward bifurcation. In order to eradicate COVID-19, it is necessary to ensure that patients can receive timely treatment.

## 4. Model analysis of COVID-19

### *4.1. Model calibration*

In this part, we perform computer simulations of the model (2.1). First, we calibrate our model to the COVID-19 data from Shanghai, China. The data is from Shanghai Municipal Health Commission [37] and National Health Commission of the People's Republic of China [38]. In 2021, the total population

of Shanghai is about 24,894,300 [39]. By February 2022, the cumulative number of confirmed cases is 4388, the number of existing cases is 510, and the cumulative number of cured cases is 3871. The detailed data is shown in Figure 2. The natural mortality rate of Shanghai in 2021 is 0.00559 [39]. Thus, we can obtain that $\mu = 0.0000153$ per day. The disease-related mortality rate is $\varepsilon = 0.00173$ [37]. $\Lambda$ can be estimated by $\mu N$, that is, $\Lambda = 381$. We don't know the exact vaccination rate in the crowd, and because the COVID-19 virus mutates, the effectiveness of the vaccine is unknown. Considering that many people who have been vaccinated have later contracted COVID-19, we chose a small value of $v = 0.00003$. In the model (2.1), the initial value is $(S(0), E(0), I(0), R(0)) = (24{,}894{,}300, 108, 480, 3863)$. Other model parameters are estimated.

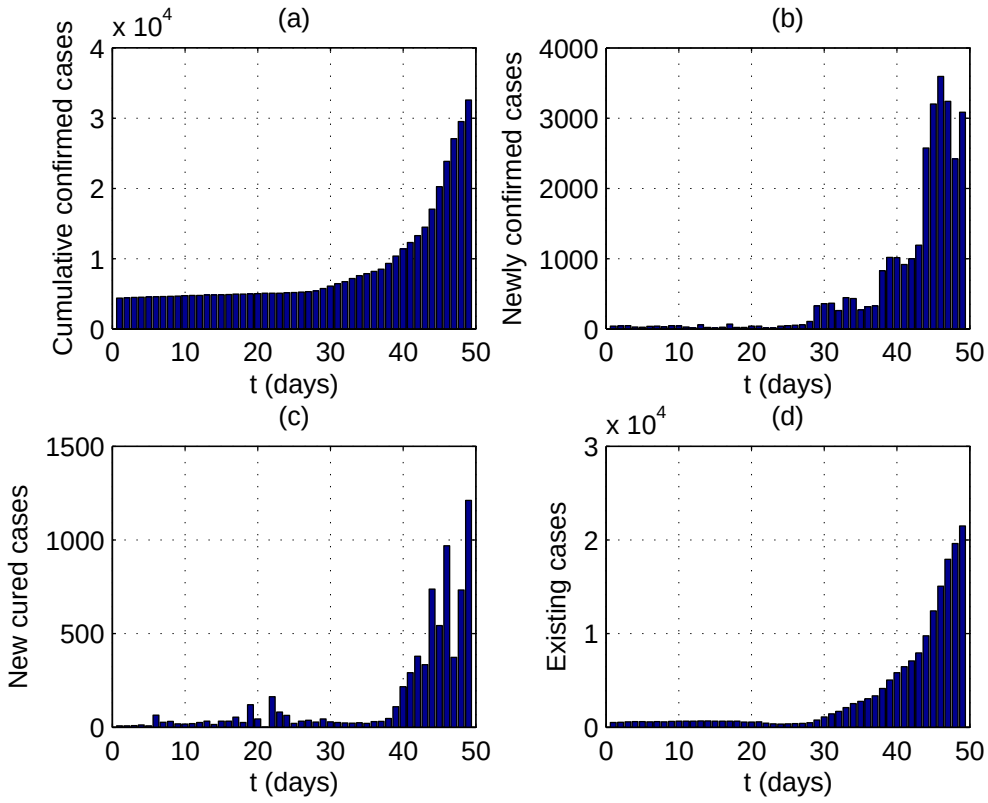


**Figure 2.** The COVID-19 data in Shanghai for 49 days starting from March 1, 2022. (a) The cumulative confirmed cases, (b) the newly confirmed cases, (c) the newly cured cases, and (d) the existing cases.

To estimate the relevant parameters, we utilize the Nelder-Mead search algorithm, one of the most renowned algorithms for solving multidimensional unconstrained nonlinear minimization problems [40], to search for the local minima of the model (2.1) with initial condition $(S(0), E(0), I(0), R(0)) = (24{,}894{,}300, 108, 480, 3863)$, and capture the relevant parameters so that the model outcome is a better fit to the real data. The fitting is done for 49 days starting from March 1, 2022. The relevant results are listed in Table 4. Figure 3 shows the output of the model and the existing infection cases, where Figure 3(a) depicts the existing cases and the output $I(t)$ of the model. From the subgraph, it can be observed that the fitting results are very close to the data. Moreover, the basic reproduction number is

$\mathscr{R}_0 = 2.3899$ in Shanghai, calculated from the parameter estimates listed in Table 4. As $\mathscr{R}_0 > 1$, the disease-free equilibrium is unstable, and COVID-19 will break out in Shanghai.

**Table 4.** Parameters fitted with data.

| Parameter | Value | Source |
|---|---|---|
| $\Lambda$ | 381 | [39] |
| $\mu$ | 0.00559/365 | [39] |
| $\varepsilon$ | 0.00173 | [37] |
| $v$ | 0.00003 | Assumed |
| $\beta_1$ | $2.585 \times 10^{-7}$ | Fitted |
| $\beta_2$ | $3.56 \times 10^{-8}$ | Fitted |
| $\delta$ | $2.64 \times 10^{-2}$ | Fitted |
| $\beta$ | $5.172 \times 10^{-3}$ | Fitted |
| $\alpha$ | $1.614 \times 10^{3}$ | Fitted |
| $b$ | $7.379 \times 10^{-3}$ | Fitted |
| $c$ | 0.8786 | Fitted |

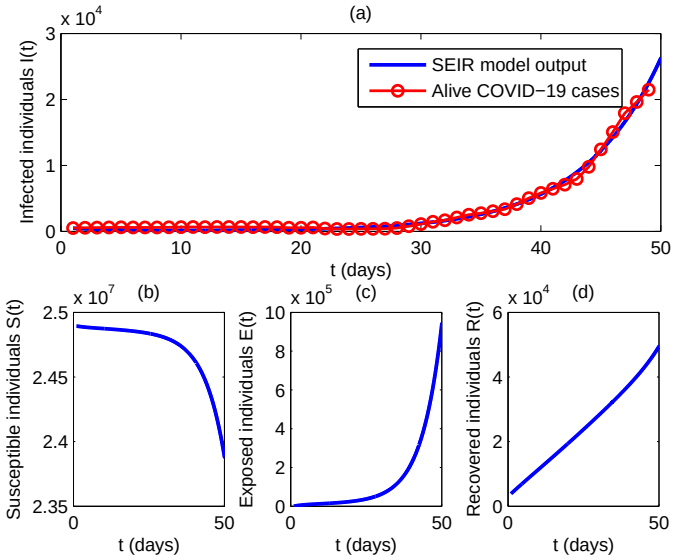


**Figure 3.** The fitting results of the model (2.1) with COVID-19 data in Shanghai for 49 days starting from March 1, 2022. The red dotted line represents the actual data points observed. The figure shows that the number of existing cases is increasing exponentially.

### *4.2. Sensitivity analysis*

To describe how to reduce the number of COVID-19 infections, it is essential to see the relative importance of various factors that lead to the spread of COVID-19. Since the initial spread of the disease is completely related to the basic reproductive number $\mathscr{R}_0$, we calculate the sensitivity index of $\mathscr{R}_0$ to the model parameters. Specifically, for parameters $\Theta = (\beta_1, \beta, \Lambda, \mu, v, c, \varepsilon, \delta)$, the normalized forward

sensitivity index vector for $\mathscr{R}_0$, say $\Upsilon$, can be calculated by

$$\Upsilon = \frac{\partial \mathscr{R}_0}{\partial \Theta} \cdot \frac{\Theta}{\mathscr{R}_0}.$$

Using the values of each relevant parameter given in Table 4, Figure 4 shows the sensitivity index of the parameters. The sensitivity index of $\mathscr{R}_0$ regarding $\beta_1$ and $\Lambda$ is 1, which indicates that these two parameters are independent of other parameters. In other words, $\mathscr{R}_0$ is an increasing function with respect to $\beta_1$ (or $\Lambda$), and if $\beta_1$ (or $\Lambda$) increases by 1%, $\mathscr{R}_0$ also increases by 1%. Obviously, the sensitivity indices of $\beta_1$, $\beta$, and $\Lambda$ are positive. It implies that $\mathscr{R}_0$ will increase with the increase of these parameters. It is worth noting that these three parameters have different degrees of impact on $\mathscr{R}_0$, among which $\beta_1$ and $\Lambda$ have a strong impact on $\mathscr{R}_0$, and $\beta$ has a weak impact on it. On the contrary, $\mu$, $v$, $c$, $\varepsilon$, and $\delta$ have negative sensitivity indices. It means that $\mathscr{R}_0$ decreases as these parameters increase. The parameters $\mu$, $v$, and $c$ strongly impact $\mathscr{R}_0$, while $\varepsilon$ and $\delta$ have a relatively weak impact.

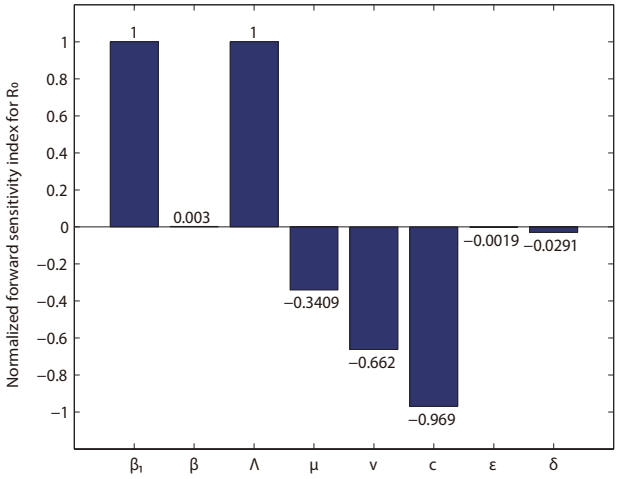


**Figure 4.** The normalized forward sensitivity indices of $\mathscr{R}_0$ with respect to the parameter values used in Table 4.

Therefore, to completely eliminate COVID-19, we must control the growth of the parameters having positive indices, especially $\Lambda$ and $\beta_1$. An effective way to control $\Lambda$, i.e., the recruitment rate of susceptible individuals, is to blockade the region and eliminate the migration of people from outside the region. However, such a measure is not a long-term solution, as it will seriously hinder the socio-economic development and cause a lot of inconvenience to people's lives. In contrast, in order to control the increase of the number of infected people, reducing the contact rate between susceptible and infected people $\beta_1$ is a very reasonable and effective method. On the one hand, this can be achieved by isolating the infected population on a small scale, and on the other hand, from the expression of $\mathcal{B}(I(t))$, it is easy to see that increasing $\beta_2$ or decreasing $\alpha$, which are the parameters related to the media reports, can help to reduce the actual contact rate between susceptible and infected people. In other words, fully utilizing media reports can make people more conscious of taking effective protection measures, thus helping to reduce the infection level. Relevant authorities should fully recognize the role of media coverage and

use the media to disseminate information on disease prevention and treatment, so that people are aware of current health problems and their possible solutions.

At the same time, the increase of the parameters having negative indices cannot be ignored, especially the cure rate $c$. As we mentioned in the introduction, the saturation level of medical resources in a region can be expressed as $c/b$. An increase in $c$ means, on the one hand, an increase in the cure rate and, on the other hand, an increase in medical resources. Both can lead to a decrease in $\mathscr{R}_0$, which in turn can lead to the extinction of the disease. Therefore, it is intuitive to conclude that adequate medical resources can help contain disease outbreaks. Additionally, as can be seen in Figure 4, widespread vaccination also helps to control disease epidemics.

### *4.3. Impact of critical parameters*

To begin, we select the parameter $v$ related to vaccination and draw the time series diagram of the infected compartment $I$ by changing the value of $v$. It is evident from Figure 5(a) that increasing the vaccination rate can significantly reduce the number of infected individuals.

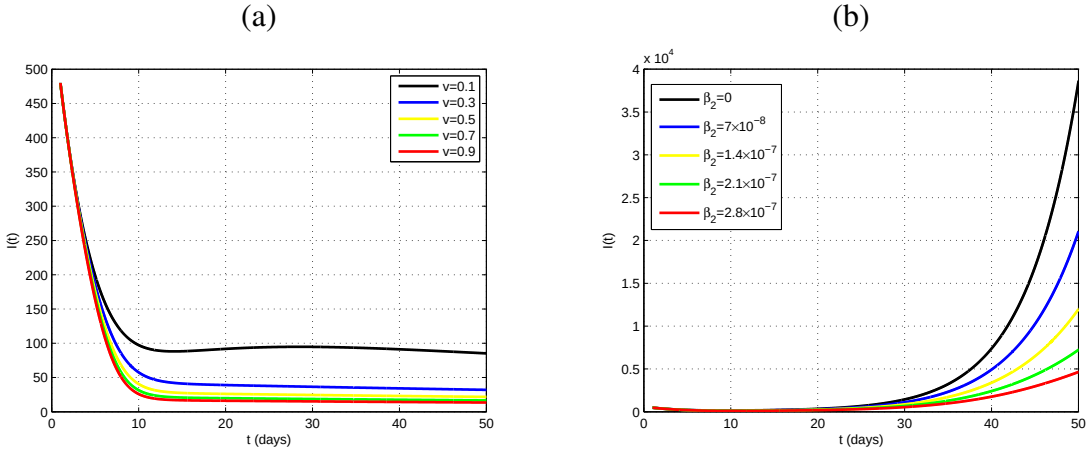


**Figure 5.** Simulation of the effect of (a) $v$ and (b) $\beta_2$ on compartment $I$.

Next, we study the impact of media coverage on the spread of COVID-19. In the introduction, two key parameters are closely related to the effects of media coverage. One is the maximum reduction in contact rate $\beta_2$ that can be achieved by media coverage, and the other is the parameter $\alpha$ that characterizes the response speed of people to media coverage. We change the values of these two parameters and plot the time series of the infected compartment $I$. Figure 5(b) shows that the curve of $I(t)$ gradually decreases. The black curve represents the trend of $I(t)$ without the influence of media coverage. The more significant the maximum reduction in contact rate achieved by media coverage, the stronger its ability to control COVID-19. Thus, it is essential to maintain intensive media coverage during the epidemic period. Figure 6 displays the trend of $I(t)$ when $\alpha$ continuously ranges from 0 to 5000. As $\alpha$ rises, so does the $I(t)$ trend, suggesting that the faster people respond to media reports, the fewer infected individuals. When $\alpha$ ranges from [0, 1000], the trend of $I(t)$ is apparent, whereas when $\alpha$ is within the range [4000, 5000], the alteration of $I(t)$ becomes less noticeable as $\alpha$ increases. When $\alpha = 0$, the level of $I(t)$ is the lowest. Although $I(t)$ does not show a trend toward 0, compared to the case where $\alpha > 0$, the number of infections is the lowest when $\alpha = 0$ at each time node. This shows that the faster

people respond to media coverage, the more conducive to reducing the prevalence of COVID-19 and keeping the number of existing cases at a low level.

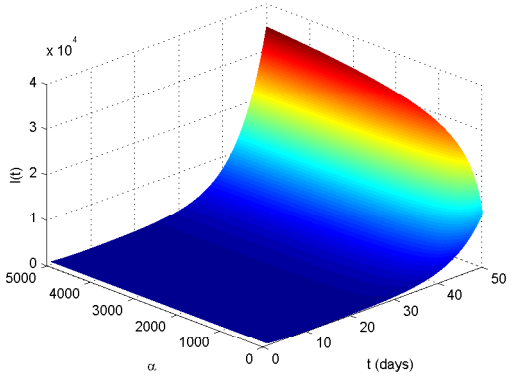


**Figure 6.** Simulation of the effect of $\alpha$ for compartment $I$.

As illustrated in Figure 7(a), when $b$ decreases, both the growth rate and the overall level of $I(t)$ decrease. This indicates that timely treatment of infected individuals can significantly reduce the number of infected individuals. As shown in Figure 7(b), the smaller the value of $c$, the faster the growth rate of $I(t)$. This suggests that increasing the cure rate can also effectively control the disease. Figure 8 presents the temporal impact of $b$ and $c$ on compartment $I(t)$. Figure 8(a) indicates that when $b$ is relatively tiny, $I(t)$ exhibits sensitivity to variations in $b$. However, Figure 8(b) demonstrates that as the parameter $c$ approaches 1, $I(t)$ experiences almost no change, while when $c$ is relatively tiny, $I(t)$ experiences significant changes.

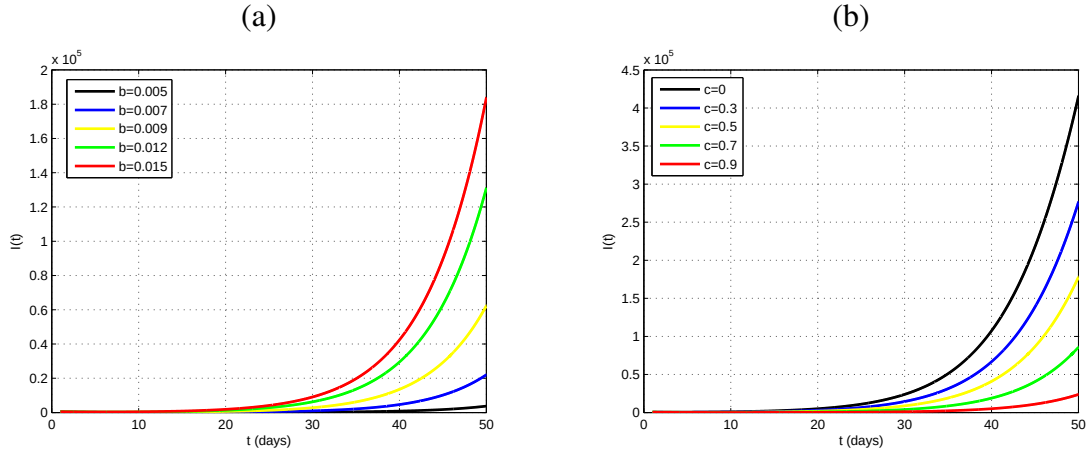


**Figure 7.** Simulation of the effect of parameters (a) $b$ and (b) $c$ on compartment $I$.

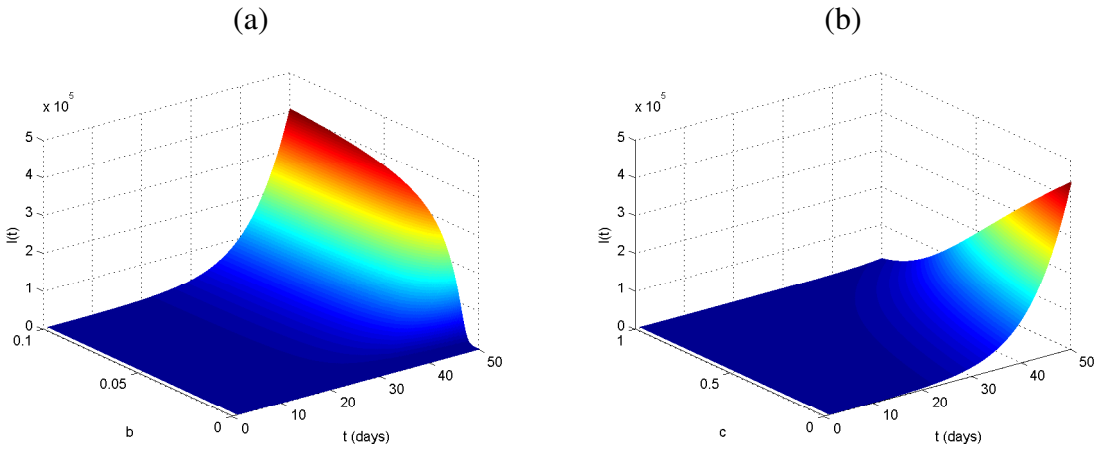


**Figure 8.** Simulation of the effect of (a) $b$ and (b) $c$ with respect to time $t$ for compartment $I$.

The number of infected individuals on the 30th day (i.e., $I(30)$) is the dependent variable to investigate the joint impact of $b$ and $c$ on $I$. The following conclusion can be drawn from Figure 9: (i) For a fixed parameter $c$ ($\neq 0$), $I(30)$ will increase as $b$ increases; (ii) for a fixed parameter $b$, $I(30)$ will decrease as $c$ increases; (iii) $I(30)$ is sensitive to both small $b$ and $c$; (iv) in order to prevent and control COVID-19, measures should be taken to increase $c$ and reduce $b$. On the one hand, larger $c$ and smaller $b$ represent timely and efficient treatment; on the other, they represent sufficient medical resource supply. Both of these aspects play an important role in curbing the epidemic.

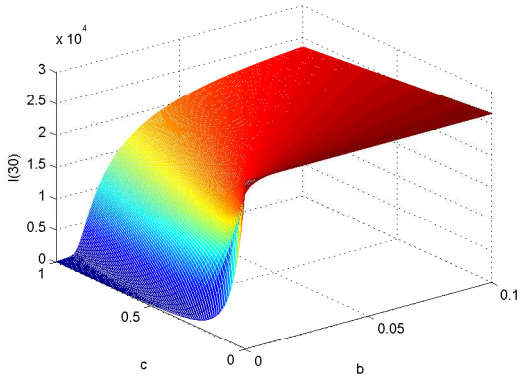


**Figure 9.** The interrelationship of $b$ and $c$ on $I$.

Figure 10(a),(b) shows the values of $\mathscr{R}_0$ when $\beta_1$ and $\beta$ change, as well as when $\beta_1$ and $c$ change, respectively. The blue surface is $\mathscr{R}_0 = 1$. Since $\mathscr{R}_0 = 2.3899 > 1$, the COVID-19 pandemic will persist. To reduce $\mathscr{R}_0$ below 1, it can be seen from Figure 10 that reducing $\beta_1$ or increasing $c$ is an effective way.

The above analysis can lead to some valuable conclusions. As is known to all, $\mathscr{R}_0$ represents the average number of secondary infections in a single infected individual. Therefore, reducing the value of $\mathscr{R}_0$ can effectively curb the development of the epidemic. From this perspective, six measures are taken. (i) Limit crowd gathering and persuade people to reduce the exposure rate. (ii) Control the prevalence of latent patients through early intervention treatment after high-risk close contact. (iii) Decrease the recruitment rate of susceptibility by closing the entire epidemic area. (iv) Increase the vaccination rate

so that most people have antibodies. (v) Improve the recovery rate of infected individuals through hospital support treatment. (vi) Ensure adequate supply of medical resources.

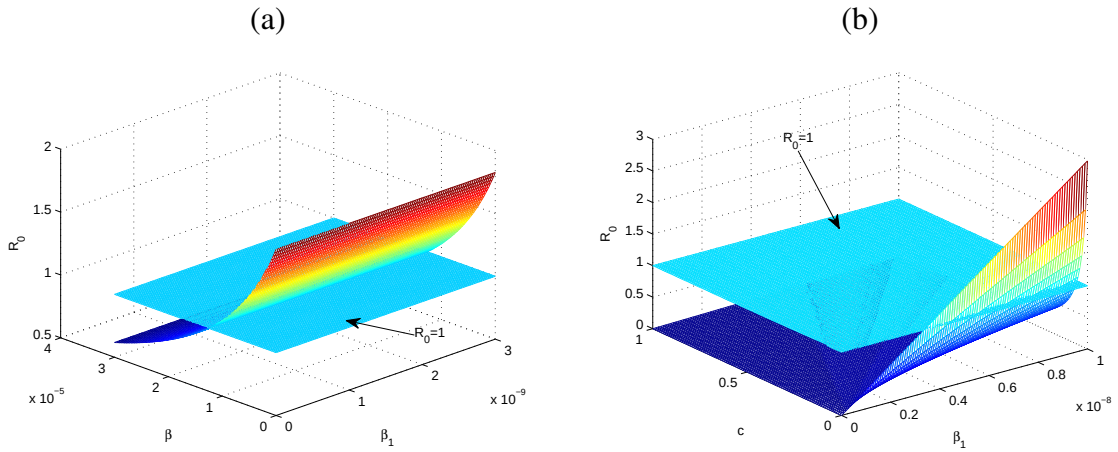


**Figure 10.** The value of $\mathscr{R}_0$ when parameter $\beta_1$ and $\beta$, $c$ varies.

### *4.4. Bifurcation analysis*

Next, we give the numerical result of the bifurcation behavior of model (2.1) using $\mathscr{R}_0$ as the bifurcation parameter. Applying the parameter values in Table 4, it can be calculated that $b^* = 6 \times 10^{-3} < b = 7.379 \times 10^{-3}$. Combining $\mathscr{R}_0 = 2.3899 > 1$, Theorem 4 (II)(i) shows that the model (2.1) has only one EEP. Meanwhile, $\hat{b} = 2.1207 \times 10^{-4} < b = 7.379 \times 10^{-3}$, which implies that model (2.1) exhibits a backward bifurcation at $\mathscr{R}_0 = 1$. Furthermore, $\Delta = -2.8168 \times 10^{20} < 0$. Hence, when $G < \mathscr{R}_0 < 1$, model (2.1) has two EEPs according to Theorem 4 (II)(ii1). Figure 11 depicts the backward bifurcation of model (2.1), confirming the analysis above. As stated in Remark 3, the emergence of backward branches makes it more difficult to control COVID-19. To avoid this situation, we can reduce the value of $b$ so that $b < \hat{b}$.

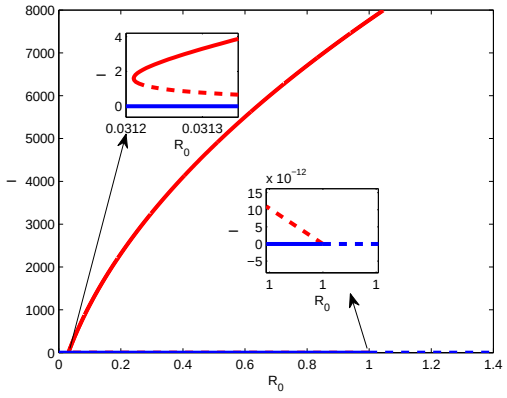


**Figure 11.** Bifurcation diagram in the plane $(\mathscr{R}_0, I)$.

### 4.5. *Long-term behavior*

The previous subsection analyzed the effect of some of the key parameters on the model from a microscopic point of view. In this subsection, we zoom in on the time scale and focus on two important factors, namely, the impact of media coverage and limited medical resources on disease transmission.

Figures 12 and 13 show the changes in the population of infected persons over time. If no intervention is made and the epidemic is allowed to develop, it will spread rapidly in Shanghai, resulting in more than 3 million infections, before the number of infected people declines slowly and eventually reaches a lower level of the epidemic (red curve). In order to study the effect of media coverage on the spread of the disease, we plotted the change in the number of infected people by choosing different values of $\beta_2$ and $\alpha$, as shown in Figure 12(a),(b). From the values of $\beta_2$, it can be clearly seen that the larger the maximum contact rate that can be reduced by media coverage, the smaller the number of infected individuals and the lower the peak value. As $\beta_2$ increases, the peak is delayed. However, changes in $\alpha$ do not have the same effect on the infected individuals as $\beta_2$, which only slightly delays the onset of the peak.

Figure 13(a),(b) shows the changes in the infected individuals with different values of $c$ and $b$. Similar to the change in $\alpha$, the change in $c$ has a smaller impact on the peak, but it can greatly delay the time of peak occurrence. The change in $b$ has a more obvious and rich dynamical behavior. On the one hand, the number of infected individuals will decrease with the decrease of $b$, and the decrease speed is very fast, while the peak also drops very fast. On the other hand, the time of peak occurrence will also be delayed.

To summarize, from a macroscopic point of view, we are inclined to take measures to make $\beta_2$ very large and $\alpha$ very small, and at the same time to make $c$ very large and $b$ very small. This would greatly reduce the number of infected individuals and delay the peak so that people have more time to deal with the threat of an epidemic.

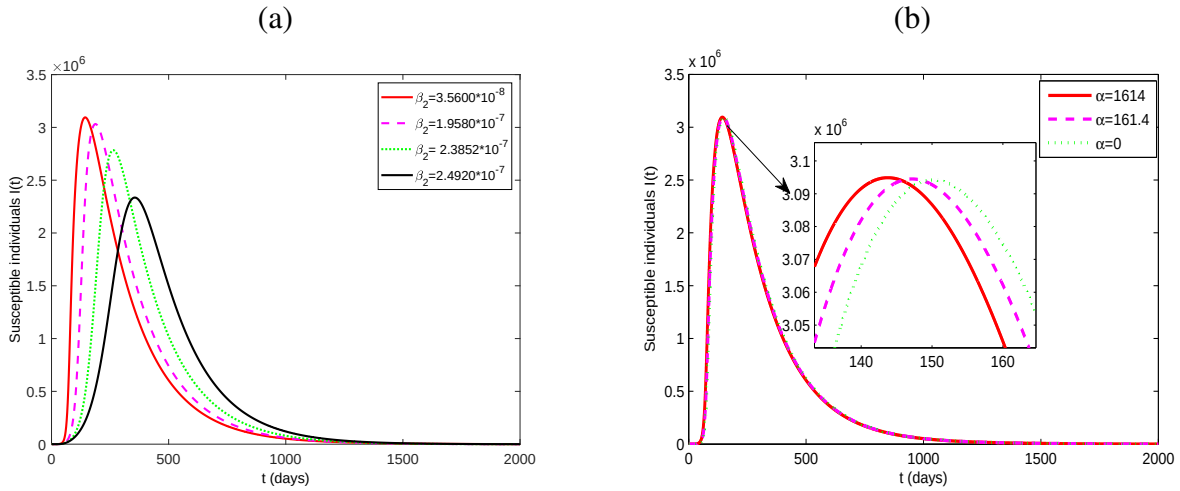


**Figure 12.** Variation of infective individuals ($I(t)$) with respect to time for different values of (a) $\beta_2$ and (b) $\alpha$. Other parameters are list in Table 4.

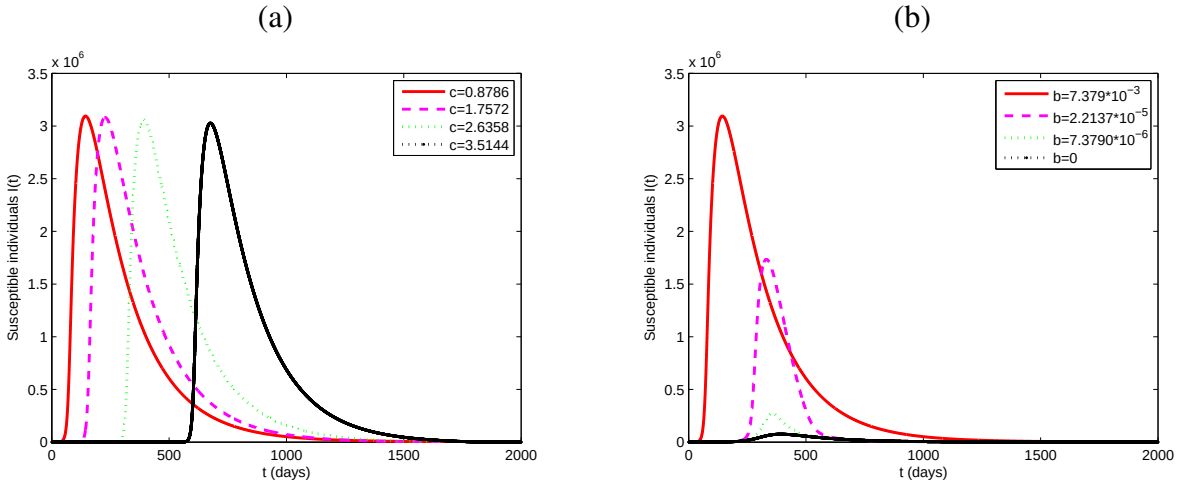


**Figure 13.** Variation of infective individuals ($I(t)$) with respect to time for different values of (a) $c$ and (b) $b$. Other parameters are list in Table 4.

## 5. Conclusions

In this paper, we propose a new SEIR model for COVID-19, which considers the impact of media coverage and limited medical resources on the spread of COVID-19. For this model, we first demonstrate the positive and boundedness of the solution. The next-generation matrix method derives the basic reproductive number $\mathscr{R}_0$. As a critical threshold, the value of $\mathscr{R}_0$ determines whether the disease will go extinct. We analyzed the equilibrium point of the model in detail and gave the distribution of equilibrium points under the two conditions of $0 \leq b \leq b^*$ and $b > b^*$. At the same time, we also explored the local stability of the equilibrium point of the endemic disease. For the bifurcation phenomenon, we proved that when $b > \hat{b}$, the model exhibits a bifurcation at $\mathscr{R}_0 = 1$.

The proposed model applies to the confirmed case data of Shanghai from March 1, 2022 to April 18, 2022. Using this data, seven important parameters were estimated. By calculating these parameters, we obtained $\mathscr{R}_0 = 2.3899$, indicating that COVID-19 will continue to spread without measures being taken. The results of the sensitivity analyses explored the importance of media coverage in reducing the spread of the disease, and also revealed that limited medical resources were an impediment to controlling the epidemic, and that only an adequate supply of medical resources could help to curb the development of the epidemic. In addition, a more comprehensive numerical analysis of some important parameters was carried out. The analysis shows that susceptible populations must be widely vaccinated and the media should maintain high-intensity coverage to influence more people. In addition, ensuring that infected people can receive timely treatment also helps to control the disease. The bifurcation analysis of the model illustrates this point, too. We also explored the changes of infected individuals over a long period of time.

The results of this study suggest that media coverage plays an important role in suppressing the spread of disease and is an effective strategy for controlling disease. Therefore, the authorities should pay attention to it. When biomedical interventions are not sufficient to protect people from disease, timely media coverage is often the best method. The limited availability of medical resources can hinder efforts to contain the disease. The authorities should try their best to ensure sufficient medical

resources, including medical personnel, medical expenses, medical institutions, medical beds, medical facilities and equipment, knowledge and skills, and information to ensure that every patient can receive timely treatment.

In the work, some problems are worth in-depth study, such as considering the influence of random environmental perturbation on the model or the the imprecision of model parameters [41]. We will focus on this in future studies.

## Use of AI tools declaration

The authors declare they have not used Artificial Intelligence (AI) tools in the creation of this article.

## Acknowledgments

This work is supported by the Research Innovation Program for Postgraduates of Xinjiang Uygur Autonomous Region under Grant (No. XJ2023G017), the National Natural Science Foundation of China (No. 12061070), the Natural Science Foundation of Xinjiang Uygur Autonomous Region of China (No. 2021D01E13), and the 2023 Annual Planning Project of Commerce Statistical Society of China under Grant (No. 2023STY61).

## Conflict of interest

The authors declare there is no conflict of interest.

## References

1. K. Sarkar, J. Mondal, S. Khajanchi, How do the contaminated environment influence the transmission dynamics of COVID-19 pandemic, *Eur. Phys. J. Spec. Top.*, **231** (2022), 3697–3716. https://doi.org/10.1140/epjs/s11734-022-00648-w
2. *World Health Organization*, Coronavirus disease (COVID-19) pandemic, 2023. Available from: https://www.who.int/emergencies/diseases/novel-coronavirus-2019.
3. W. O. Kermack, A. G. McKendrick, A contribution to the mathematical theory of epidemics, *Proc. R. Soc. Lond. A*, **115** (1927), 700–721. https://doi.org/10.1098/rspa.1927.0118
4. L. Zhou, M. Fan, Dynamics of an SIR epidemic model with limited medical resources revisited, *Nonlinear Anal. Real World Appl.*, **13** (2012), 312–324. https://doi.org/10.1016/j.nonrwa.2011.07.036
5. R. George, N. Gul, A. Zeb, Z. Avazzadeh, S. Djilali, S. Rezapour, Bifurcations analysis of a discrete time SIR epidemic model with nonlinear incidence function, *Results Phys.*, **38** (2022), 105580. https://doi.org/10.1016/j.rinp.2022.105580
6. R. M. Anderson, R. M. May, Population biology of infectious diseases: Part I, *Nature*, **280** (1979), 361–367. https://doi.org/10.1038/280361a0
7. Z. Hu, P. Bi, W. Ma, S. Ruan, Bifurcations of an SIRS epidemic model with nonlinear incidence rate, *Discrete Contin. Dyn. Syst. Ser. B*, **15** (2011), 93–112. https://doi.org/10.3934/dcdsb.2011.15.93

8. A. Lahrouz, L. Omari, D. Kiouach, A. Belmaâti, Complete global stability for an SIRS epidemic model with generalized non-linear incidence and vaccination, *Appl. Math. Comput.*, **218** (2012), 6519–6525. https://doi.org/10.1016/j.amc.2011.12.024

9. S. Gao, H. Ouyang, J. J. Nieto, Mixed vaccination strategy in SIRS epidemic model with seasonal variability on infection, *Int. J. Biomath.*, **4** (2011), 473–491. https://doi.org/10.1142/S1793524511001337

10. J. Li, Z. Ma, Global analysis of SIS epidemic models with variable total population size, *Math. Comput. Modell.*, **39** (2004), 1231–1242. https://doi.org/10.1016/j.mcm.2004.06.004

11. Y. Li, J. Cui, The effect of constant and pulse vaccination on SIS epidemic models incorporating media coverage, *Commun. Nonlinear Sci. Numer. Simul.*, **14** (2009), 2353–2365. https://doi.org/10.1016/j.cnsns.2008.06.024

12. M. E. Fatini, A. Lahrouz, R. Pettersson, A. Settati, R. Taki, Stochastic stability and instability of an epidemic model with relapse, *Appl. Math. Comput.*, **316** (2018), 326–341. https://doi.org/10.1016/j.amc.2017.08.037

13. Y. Ding, Y. Fu, Y. Kang, Stochastic analysis of COVID-19 by a SEIR model with Lévy noise, *Chaos: Interdiscip. J. Nonlinear Sci.*, **31** (2021), 043132. https://doi.org/10.1063/5.0021108

14. M. Cai, G. E. Karniadakis, C. Li, Fractional SEIR model and data-driven predictions of COVID-19 dynamics of Omicron variant, *Chaos: Interdiscip. J. Nonlinear Sci.*, **32** (2022), 071101. https://doi.org/10.1063/5.0099450

15. E. F. D. Goufo, C. Ravichandran, G. A. Birajdar, Self-similarity techniques for chaotic attractors with many scrolls using step series switching, *Math. Modell. Anal.*, **26** (2021), 591–611. https://doi.org/10.3846/mma.2021.13678

16. C. Ravichandran, K. Logeswari, A. Khan, T. Abdeljawad, J. F. Gómez-Aguilar, An epidemiological model for computer virus with Atangana-Baleanu fractional derivative, *Results Phys.*, **51** (2023), 106601. https://doi.org/10.1016/j.rinp.2023.106601

17. K. S. Nisar, K. Logeswari, V. Vijayaraj, H. M. Baskonus, C. Ravichandran, Fractional order modeling the gemini virus in capsicum annuum with optimal control, *Fractal Fract.*, **6** (2022), 61. https://doi.org/10.3390/fractalfract6020061

18. K. Sarkar, S. Khajanchi, J. J. Nieto, Modeling and forecasting the COVID-19 pandemic in India, *Chaos, Solitons Fractals*, **139** (2020), 110049. https://doi.org/10.1016/j.chaos.2020.110049

19. S. Khajanchi, K. Sarkar, Forecasting the daily and cumulative number of cases for the COVID-19 pandemic in India, *Chaos: Interdiscip. J. Nonlinear Sci.*, **30** (2020), 071101. https://doi.org/10.1063/5.0016240

20. P. Samui, J. Mondal, S. Khajanchi, A mathematical model for COVID-19 transmission dynamics with a case study of India, *Chaos, Solitons Fractals*, **140** (2020), 110173. https://doi.org/10.1016/j.chaos.2020.110173

21. S. Khajanchi, K. Sarkar, J. Mondal, K. S. Nisar, S. F. Abdelwahab, Mathematical modeling of the COVID-19 pandemic with intervention strategies, *Results Phys.*, **25** (2021), 104285. https://doi.org/10.1016/j.rinp.2021.104285

22. R. K. Rai, P. K. Tiwari, S. Khajanchi, Modeling the influence of vaccination coverage on the dynamics of COVID-19 pandemic with the effect of environmental contamination, *Math. Methods Appl. Sci.*, **46** (2023), 12425–12453. https://doi.org/10.1002/mma.9185
23. N. Anggriani, M. Z. Ndii, R. Amelia, W. Suryaningrat, M. A. A. Pratama, A mathematical COVID-19 model considering asymptomatic and symptomatic classes with waning immunity, *Alexandria Eng. J.*, **61** (2022), 113–124. https://doi.org/10.1016/j.aej.2021.04.104
24. X. Lü, H. W. Hui, F. F. Liu, Y. L. Bai, Stability and optimal control strategies for a novel epidemic model of COVID-19, *Nonlinear Dyn.*, **106** (2021), 1491–1507. https://doi.org/10.1007/s11071-021-06524-x
25. R. K. Rai, S. Khajanchi, P. K. Tiwari, E. Venturino, A. K. Misra, Impact of social media advertisements on the transmission dynamics of COVID-19 pandemic in India, *J. Appl. Math. Comput.*, **68** (2022), 19–44. https://doi.org/10.1007/s12190-021-01507-y
26. G. P. Sahu, J. Dhar, Dynamics of an SEQIHRS epidemic model with media coverage, quarantine and isolation in a community with pre-existing immunity, *J. Math. Anal. Appl.*, **421** (2015), 1651–1672. https://doi.org/10.1016/j.jmaa.2014.08.019
27. R. Liu, J. Wu, H. Zhu, Media/psychological impact on multiple outbreaks of emerging infectious diseases, *Comput. Math. Methods Med.*, **8** (2007), 153–164. https://doi.org/10.1080/17486700701425870
28. J. Pang, J. A. Cui, An SIRS epidemiological model with nonlinear incidence rate incorporating media coverage, in *2009 Second International Conference on Information and Computing Science*, Manchester, UK, **3** (2009), 116–119. https://doi.org/10.1109/ICIC.2009.235
29. I. Ghosh, P. K. Tiwari, S. Samanta, I. M. Elmojtaba, N. Al-Salti, J. Chattopadhyay, A simple SI-type model for HIV/AIDS with media and self-imposed psychological fear, *Math. Biosci.*, **306** (2018), 160–169. https://doi.org/10.1016/j.mbs.2018.09.014
30. A. K. Misra, A. Sharma, J. B. Shukla, Stability analysis and optimal control of an epidemic model with awareness programs by media, *Biosystems*, **138** (2015), 53–62. https://doi.org/10.1016/j.biosystems.2015.11.002
31. C. Maji, F. A. Basir, D. Mukherjee, K. S. Nisar, C. Ravichandran, COVID-19 propagation and the usefulness of awarenessbased control measures: A mathematical model with delay, *AIMS Math.*, **7** (2022), 12091–12105. https://doi.org/10.3934/math.2022672
32. S. Khajanchi, K. Sarkar, J. Mondal, Dynamics of the COVID-19 pandemic in India, preprint, arXiv:2005.06286v2. https://doi.org/10.48550/arXiv.2005.06286
33. W. Wang, S. Ruan, Bifurcations in an epidemic model with constant removal rate of the infectives, *J. Math. Anal. Appl.*, **291** (2004), 775–793. https://doi.org/10.1016/j.jmaa.2003.11.043
34. W. Wang, Backward bifurcation of an epidemic model with treatment, *Math. Biosci.*, **201** (2006), 58–71. https://doi.org/10.1016/j.mbs.2005.12.022
35. X. Zhang, X. Liu, Backward bifurcation of an epidemic model with saturated treatment function, *J. Math. Anal. Appl.*, **348** (2008), 433–443. https://doi.org/10.1016/j.jmaa.2008.07.042
36. C. Castillo-Chavez, B. Song, Dynamical models of tuberculosis and their applications, *Math. Biosci. Eng.*, **1** (2004), 361–404. https://doi.org/10.3934/mbe.2004.1.361

37. *Shanghai Municipal Health Commission*, Prevention and control of COVID-19, 2022. Available from: https: //wsjkw.sh.gov.cn/yqfk2020/.

38. *National Health Commission of the People's Republic of China*, Prevention and control of the COVID-19 epidemic, 2022. Available from: http://www.nhc.gov.cn/xcs/xxgzbd/gzbd_index. shtml.

39. *National Bureau of Statistics*, China Statistical Yearbook, 2022. Available from: http://www.stats.gov. cn/sj/ndsj/.

40. J. C. Lagarias, J. A. Reeds, M. H. Wright, P. E. Wright, Convergence properties of the Nelder–Mead simplex method in low dimensions, *SIAM J. Optim.*, **9** (1998), 112–147. https://doi.org/10.1137/S1052623496303470

41. S. Bera, S. Khajanchi, T. K. Roy, Stability analysis of fuzzy HTLV-I infection model: A dynamic approach, *J. Appl. Math. Comput.*, **69** (2023), 171–199. https://doi.org/10.1007/s12190-022-01741-y


AIMS Press